

# SZ effect or Not? - Detecting most galaxy clusters' main foreground effect

Weike Xiao<sup>1\*</sup>, Chen Chen<sup>2</sup>, Bin Zhang<sup>2</sup>, Yongfeng Wu<sup>3†</sup>, Mi Dai<sup>4</sup>

<sup>1</sup>*Department of Astronautics Engineering, Harbin Institute of Technology, Heilongjiang Province, China, 150001*

<sup>2</sup>*Department of Physics, Harbin Institute of Technology, Heilongjiang Province, China, 150001*

<sup>3</sup>*American Physical Society, Maryland, USA*

<sup>4</sup>*Homer L. Dodge Department of Physics and Astronomy, University of Oklahoma, Norman, OK 73019 USA*

14 January 2021

## ABSTRACT

Galaxy clusters are the most massive objects in the Universe and comprise a high-temperature intracluster medium of about  $10^7$  K, believed to offer a main foreground effect for cosmic microwave background (CMB) data in the form of the thermal Sunyaev-Zeldovich (SZ) effect. This assumption has been confirmed by SZ signal detection in hundreds of clusters but, in comparison with the huge numbers of clusters within optically selected samples from Sloan Digital Sky Survey (SDSS) data, this only accounts for a fewer cent of clusters. Here we introduce a model-independent new method to confirm the assumption that most galaxy clusters can offer the thermal SZ signal as their main foreground effect. For the *Wilkinson Microwave Anisotropy Probe* (WMAP) seven-year data (and a given galaxy cluster sample), we introduced a parameter  $d_1$  as the nearest-neighbour cluster angular distance of each pixel, then we classified data pixels as to be ( $d_1 \rightarrow 0$  case) or not to be ( $d_1$  large enough) affected by the sample clusters. By comparing the statistical results of these two kinds of pixels, we can see how the sample clusters affect the CMB data directly. We find that the *Planck* Early Sunyaev-Zeldovich (ESZ) sample and X-ray samples ( $10^2$  clusters) can lead to obvious temperature depression in the *WMAP* seven-year data, which confirms the SZ effect prediction. However, each optically selected sample ( $> 10^4$  clusters) shows an opposite result: the mean temperature rises to about  $10\mu$  K. This unexpected qualitative scenario implies that the main foreground effect of most clusters is *not* always the expected SZ effect. This may be the reason why the SZ signal detection result is lower than expected from the model.

**Key words:** methods: statistical C galaxies: clusters: general C cosmic background radiation.

## 1 INTRODUCTION

As the most massive self-gravitating systems in the cosmos, galaxy clusters can make significant contributions to the measurements of precision cosmology and, during their formation and evolution, various effects can be analysed statistically. One such major effect is the Sunyaev-Zeldovich (SZ) effect (Sunyaev-Zel'dovich 1972): cosmic microwave background (CMB) photons can undergo inverse Compton scattering off high-energy electrons in the intracluster medium (ICM) when passing through clusters. The thermal SZ effect is considered to be a most remarkable effect, as it can increase photon energy statistically and noticeably distort the

CMB spectrum. The thermal SZ effect decreases intensity at low frequencies (like the Q, V and W bands of WMAP) and increases intensity at high frequencies.

This predictable distortion of CMB data is recognized as a marked signal of clusters. After the SZ signal of residential clusters was confirmed, blind sky surveys using the SZ effect continued over the last decade, including those of the South Pole Telescope (SPT: Carlstrom et al. 2011), Atacama Cosmology Telescope (ACT: Arthur Kosowsky et al. 2006), Planck (Planck 2006) and others. A number of high-redshift clusters are expected to be found via blind SZ sky surveys using features of the SZ signal and its insensitive properties with red shift (Carlstrom. et al. 2002). This provides a solid foundation for the measurement requirements of precision cosmology.

\* E-mail: wkxiao@hit.edu.cn

† E-mail: yongfeng.wu@maine.edu

Here we note that a basic assumption is behind the expectations of these ongoing projects: the main foreground effect of most galaxy clusters on CMB data should be the expected thermal SZ effect. Although SZ signals of hundreds of clusters have already been detected and confirmed, we cannot assume that such signals exist for all clusters. In comparison with the huge cluster numbers in optically selected samples from Sloan Digital Sky Survey (SDSS) data, the basic assumption has only been validated in a few percent of clusters (and it is hard to provide their selection function: see Planck Collaboration. 2011a). Considering that unknowns can have unpredictable or unforeseen impacts on understanding or applying the results of SZ effect galaxy cluster surveys, we therefore need a means of direct detection (but not using 1.4-GHz data to analyse the 150-GHz case) of most (large percent) clusters to confirm this assumption.

At the same time, cosmological analysis methods such as the 'cluster number count'(Gilbert Holder et al. 2001; M. Manera et al. 2006) expect a complete catalogue of setting conditions. It is important to ensure that SZ-effect blind surveys of galaxy clusters do not miss cluster samples. However, some studies have already found the observed SZ-effect signal to be (especially for optically selected clusters) not strong enough (Bielby et al. 2007; Lieu et al. 2006; Planck Collaboration. 2011c; Diego et al. 2003; P. Draper et al. 2012; Neelima Sehgal et al. 2013), although this is still in debate (Planck Collaboration. 2011b; Niayesh Afshordi et al. 2007; Melin 2011). The existence and negligibility of SZ-effect signals is becoming a noteworthy debate. We note that some traditional analysis methods are model-dependent and that the free parameters can lead to uncertainty in the debate. It is therefore necessary to introduce a new model-independent method that will ensure more reliable conclusions can be drawn.

## 2 METHODS

To study foreground effects of galaxy clusters, one can consider the viewpoint of CMB data pixels, simply taking each pixel as a probe. For one galaxy cluster in an ideal isotropy CMB, a simple method is used to compare the probe data (temperature data of this pixel) of angular regions affected and unaffected by the cluster. For real CMB data, the fluctuation temperature of each pixel can be taken as another Gaussian distribution error of the detector. Considering the different properties of noise signals and the SZ signal, one can use statistical methods to compare the mean probe data of angular regions considered 'to be' or 'not to be' affected by the sample clusters. The noise signal will have similar effects on these two kinds of pixels, but the thermal SZ signal will only depress the temperature of 'to be' affected pixels.

The preconditions here are twofold: first that we are able to differentiate these two angular regions and secondly that each region includes enough data pixels to minimize the statistical error.

We find that a continuous parameter  $d_1$  is competent for such taxonomy. For each CMB data pixel,  $d_1$  is defined as the angular distance of this pixel to its nearest-neighbour galaxy cluster (of the cluster sample used). Comparison with the traditional 'stacking method' can help us to understand the parameter  $d_1$ . The stacking method selects each clus-

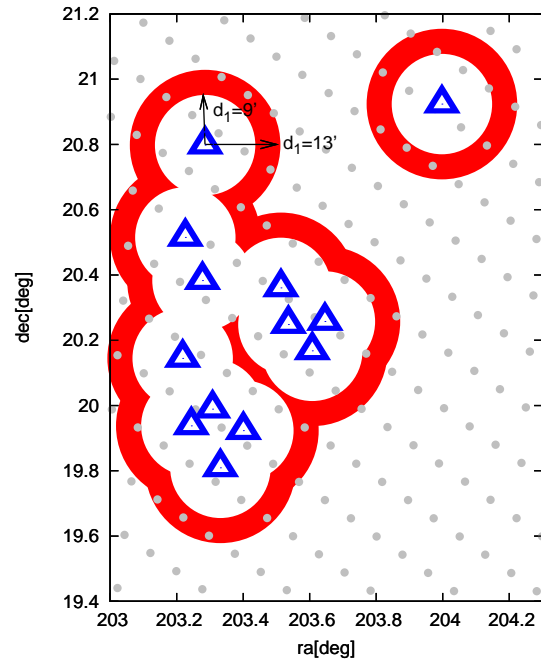


**Figure 1.** Pixel region round a group of clusters within a bin value of  $9' < d_1 < 13'$ . Each triangle corresponds to the position of one cluster in the GMBCG sample and each grey disc denotes the central position of one pixel in the WMAP data. For the sparse cluster sample (the top right one), we can see that our method will simply regress to the stacking method.

ter as the origin and bins pixels by circular rings around it (with different angular distances), using the stacking annulus of all clusters to perform analysis. Considering that galaxy clusters tend to swarm together, the temperature signal of pixels within an annulus around one cluster can be seriously affected by neighbouring clusters. In Fig.1, we show the pixel region around a group of clusters within a bin value of  $d_1$ . Our method can be comprehended as changing the circle annulus around each cluster with curved loops around the collection of sample clusters and redefining the angular parameter as  $d_1$ . This means that the angular distance to the whole cluster sample is used, rather than those for each cluster.

As clusters mainly affect their local angular region, pixels with  $d_1$  parameter large enough can properly represent the 'not to be' affected angular regions, unlike the stacking method. One other technical merit here is the impartial use of pixel data, as the stacking method applies pixels affected by neighbour clusters more times. When the cluster sample is sparse in the sky, our method simply reverts to the stacking method.

Here we illustrate the results with the optically selected Gaussian Mixture Brightest Cluster Galaxy (GMBCG:Jiangang Hao et al. 2010) galaxy cluster sample. In Fig.2, we show the distribution function of the pixel  $d_1$  parameter. This figure shows that the effective statistical region is within  $0 < d_1 < 40'$ . By comparing the possible angular size within which one cluster might affect pixel data (mainly the beam size), one can see that both cluster-affected and cluster-unaffected regions contain enough pixels for effective statistical analysis. In contrast, due to the an-

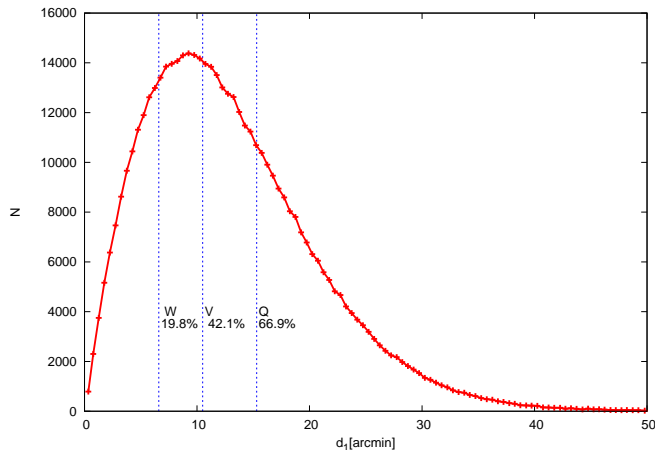


**Figure 2.** The distribution function of pixel  $d_1$  parameter. The pixels correspond to the CMB data within the main angular region of the GMBCG sample. We select the 50 580 clusters of the sample in the main survey area of SDSS DR-7 and take 503 740 *WMAP* data pixels within the area as our statistical CMB angular region. In order to avoid some unwanted edge effects, we have already dropped pixels close to the edge within 70 arcmin. The dotted lines (blue in the online article) show the beam size of *WMAP* data in the Q, V and W band, respectively, and the percentages are the proportions of pixels with  $d_1$  values within these half beam sizes.

gular resolution of *WMAP* data, this is difficult to do with SDSS galaxy samples.

We can analyse the  $\langle T \rangle - \langle d_1 \rangle$  curve (hereafter TD curve) by taking each pixel as a probe and comparing the mean temperature  $\langle T \rangle$  of pixels binned with different  $d_1$  values. The merits of this method will be discussed in detail in another article. Here, we emphasize two points relating to the physics.

First, the two sides of the TD curve represent different cases of pixels being affected or unaffected (by the cluster sample used). The main foreground effects of galaxy clusters that we are interested in (such as the SZ effect and radio emission) have the property of 'angular localization', which means that they only affect the angular region they appear in (within several arcmin for most clusters). Since the beam angle of *WMAP* data in Q, V and W bands and Internal Linear Combination (ILC) data ranges from 13 arcmin to about 30 arcmin, it is safe to say that pixels of  $d_1 \rightarrow 40'$  represent angular regions 'surely unaffected' and that  $d_1 \sim 0'$  pixels represent 'affected regions', judging by the cluster samples. By comparing the mean temperatures of these two cases, we can see how galaxy clusters affect CMB data directly.

Secondly, some background or foreground unrelated objects outside the cluster sample might also affect the CMB data, but statistically they will change both sides of the TD curve in the same way. This can be tested by simulation. Thus, if a reliable difference between the two sides is confirmed, it should be an effect caused by the cluster sample itself.

Now we can see the qualitative scenario as regards how the cluster sample affects the TD curve. When the thermal SZ effect is the main foreground effect, the mean temperature of *WMAP* data in Q, V and W bands should decline noticeably for cluster regions ( $d_1 \rightarrow 0'$ ) and the large  $d_1$

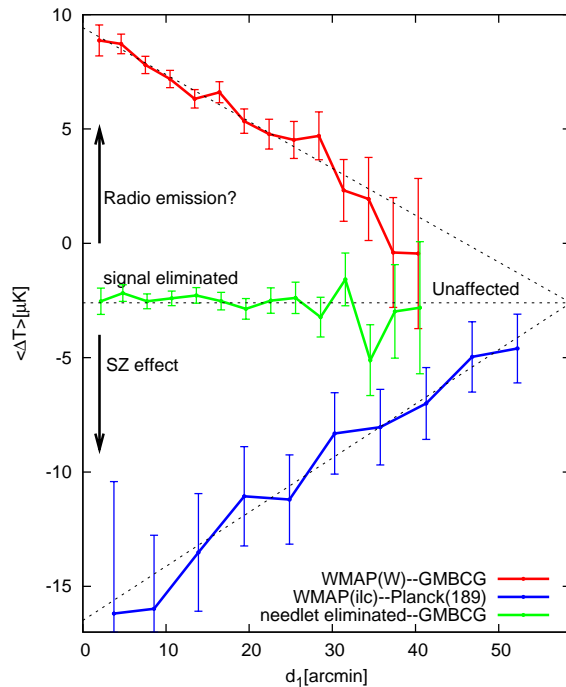


**Figure 3.** Comparison of the mean temperature of pixels with different  $d_1$  parameters. The figure shows typical TD curves of different CMB data galaxy cluster samples. The temperature distribution function of pixels within each  $d_1$  bin ( $3'$ ) can be well described with a Gauss function and we calculate the error bar of  $\langle T \rangle$

with  $\sigma = \sqrt{\frac{\sum (T_i - \langle T \rangle)^2}{N(N-1)}}$  ( $N$  is the pixel number within the  $d_1$  bin). The curves can be described with an empirical line function:  $\langle T \rangle = A * \langle d_1 \rangle + T_1$  (fitting with weight  $\sqrt{N}$ ). The traditional stack method is somehow our special case when the cluster sample is sparse and the neighbour-cluster effect can be neglected, as is the case for the Planck-189 sample. For the Planck-189 sample, we select *WMAP* data pixels round each cluster within  $55'$  as our statistical region (the bin width is  $5.5'$ ). Since only the slope  $A$  is really interesting, the *WMAP*(ILC).*Planck*(189) cluster TD curve is translated as  $\langle T \rangle - 13\mu K$  here, to show more clear contrast with the same  $\langle T \rangle$  in the unaffected region.

side should remain unaffected; then, the TD curve should rise from  $d_1 = 0'$  to  $d_1 = 40'$ . In contrast, if radio emission were the main foreground effect then the low  $d_1$  side would be driven up and the TD curve would decline.

### 3 RESULTS

In Fig.3, we illustrate the TD curve of the optically selected GMBCG sample (Jiangang Hao et al. 2010) and 189 Planck SZ-effect selected clusters (Planck-189:Planck Collaboration. 2011a). For the Planck-189 sample, the TD curve line is obviously rising, which means  $\langle T \rangle$  is much lower when  $d_1 \rightarrow 0'$  than in the large  $d_1$  region, thus indeed confirming the SZ-effect prediction. However, when the foreground is changed to the 50 580 clusters of the GMBCG sample, we obtain an unexpected opposite result: the TD curve becomes a visible downward curve, which means that the mean temperature behind clusters has an in-

CMB-cluster	$N_{cluster}$	$\Delta T_A \equiv -A * 40'$	$\Delta A/A$
WMAP(W)-GMBCG	50580	8.2 $\mu$ K	6.9 %
WMAP(V)-GMBCG	50580	6.5 $\mu$ K	8.9 %
WMAP(Q)-GMBCG	50580	7.3 $\mu$ K	4.5 %
WMAP(ilc)-GMBCG	50580	6.9 $\mu$ K	5.0 %
WMAP(W)-Wen	83279	6.3 $\mu$ K	20.3 %
WMAP(W)-maxBCG	13823	5.3 $\mu$ K	21.7 %
WMAP(W)-ACT	23	-19.4 $\mu$ K	25.1 %
WMAP(ilc)-ACT	23	-11.5 $\mu$ K	17.3 %
WMAP(W)-Planck(189)	189	-23.5 $\mu$ K	25.0 %
WMAP(ilc)-Planck(189)	189	-9.5 $\mu$ K	7.0 %
WMAP(W)-xcs3	503	-7.9 $\mu$ K	32.2 %
WMAP(ilc)-xcs3	503	-6.8 $\mu$ K	15.3 %
WMAP(W)-MCXC	1743	-7.7 $\mu$ K	23.6 %

**Table 1.** Fitting results of different samples.

crement up to about  $10\mu$ K. This result is similar for *WMAP* data in Q, V and W bands and also the ILC data, with small error margins (while the TD curve becomes a nearly level line when we use the CMB data eliminated by another team (J.Delabrouille et al. 2009) using the needlet method.)

As a post hoc examination, we also calculated the TD curves using the simulated CMB data of *WMAP* and also the simulated random distribution cluster sample. For these, no causal relationship data were found; Fig.4 shows that their TD curves are common, level curves as expected.

Fig. 3 also shows us that the TD curves of different samples are typically approximately straight lines, so we can describe them with an empirical line function:

$$\langle T \rangle = A * \langle d_1 \rangle + T_1$$

If we are not using one all-sky cluster sample, the parameter  $T_1$  can be influenced by the cluster sample region and also large-scale CMB fluctuation. The  $A$  slope is a valuable parameter. For the samples we used, the value  $\Delta T_A \equiv -A * 40'$  can show us roughly the difference of  $\langle T \rangle$  between affected and unaffected regions, which underlies how these cluster samples affect CMB data.  $\Delta T_A < 0$  corresponds to the results of the thermal SZ effect and  $\Delta T_A > 0$  relates to an opposite effect like radio emissions.

In Table 1 we show the value of  $\Delta T_A$  when setting different cluster samples as the foreground of the *WMAP* seven-year data (B. Gold et al. 2011: W band and ILC data). Here we can see the  $\Delta T_A$  values fall explicitly into two situations: for SZ-effect-selected and X-ray-selected cluster samples (ACT: Tobias A. Marrige 2011; Planck-189:Planck Collaboration. 2011a; XMM Cluster Survey (XCS-DR1):Mehrtens N. et al. 2012; Meta-Catalogue of X-ray detected Clusters of galaxies (MCXC): Piffaretti et al. 2011))  $\Delta T_A$  is obviously negative, confirming the SZ-effect image; yet for each optically selected cluster sample (GMBCG: Jiangang Hao et al. 2010; Wen: Wen et al. 2012; maxBCG: Koester et al. 2007) the  $\Delta T_A$  value is significantly positive.

In summary, with the statistical method of  $d_1$  parameters we can sum up the exponential foreground effect of galaxy clusters in these qualitative points.

(i) In angular regions of galaxy clusters, we can see the

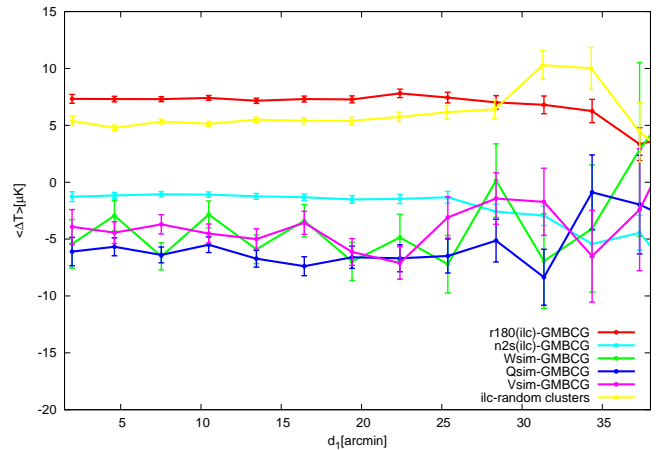


**Figure 4.** The TD curves of testing data of CMB and clusters. This figure includes (1) a randomized cluster sample (of GMBCG); (2) simulated CMB data in Q, V and W bands; (3) a reversal of CMB ILC data r180 ( $ra \rightarrow ra+180^\circ$ ), n2s ( $dec \rightarrow -dec$ ). For all the CMB data, we select the 503 740 pixels within GMBCG's main region. (Since we are not using all-sky pixels, we note that their mean temperature is not zero.)

main foreground effect is NOT the thermal SZ effect, but rather there exists an opposite contamination foreground effect somewhat like radio emission. Such an opposite signal in most clusters is high enough that it can cover the SZ-effect signal of the cluster and act as the main foreground effect. It should not be neglected when performing CMB signal analysis (whether the cluster samples are surely clusters or not).

(ii) With regard to distance, this contamination should come from the cluster itself, because if it affects the line of sight before or after the cluster, such as is the case for a star burst galaxy at high redshift background, then statistically there should also be the same effect in non-cluster regions and a temperature change should not result.

(iii) In spectra, such 'emission components' show similar effects in Q, V and W bands, a little lower at the V frequency.

## 4 DISCUSSION AND CONCLUSIONS

Before performing a quantitative study about  $\Delta T_A$  values in more detail, we focus on the explicit  $\Delta T_A > 0$  property of each optically selected cluster sample. Its value is about zero when we use a randomly distributed foreground sample in Fig.4, so it is interesting to understand why  $\Delta T_A$  changes in Fig. 3.

One might imagine that a few bright radio point sources within these samples make the mean temperature positive. Traditional cross-correlation analyses (Neelima Sehgal et al. 2013) have found that only a few percent of clusters might be affected by a nearby radio source. Here we show similar results with  $d_1$  parameter analysis between the GMBCG sample and the radio sources of Very Large Array (VLA) Faint Images of the

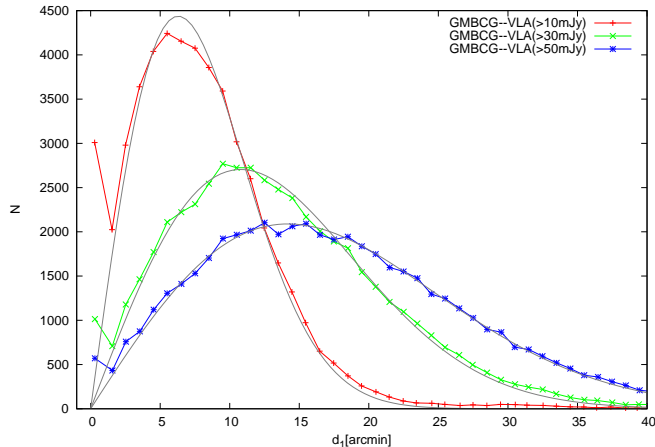


**Figure 5.** The  $d_1$  distribution curves of GMBCG sample with respect to VLA samples. Here  $d_1$  is defined as the angular distance of each GMBCG cluster's nearest-neighbourhood VLA FIRST Survey (1.4 GHz) sample. We choose flux threshold cuts of 50, 30 and 10 mJy at 1.4 GHz to yield bright radio sources at high frequency. We also fit the  $d_1 > 1'$  bins with a model of random distribution in VLA sample number density.

Radio Sky at Twenty centimetres (FIRST) catalogues<sup>1</sup> (Becker, White & Helfand 1995). In the  $d_1 \rightarrow 0$  case, Fig. 5 shows that some radio sources are surely at the cluster region, but only a few percent in total. The results for the  $d_1 > 1'$  part can be well-fitted with a random-distribution model of VLA source number density. Remember that such randomly distributed sources affect both sides of the TD curve in the same way, so radio-loud sources will not cause a  $\Delta T_A$  change.

Here we suggest that this is the result of galaxy radio emissions. The TD curve compares angular regions that are 'galaxy-rich' (cluster region) and 'hold few galaxies' (no-cluster region), so it can also represent such emissions. Each galaxy is also a diffuse foreground object affecting the observation results with similar spectra like the Galaxy (see fig. 22 in the WMAP nine-year data: Bennett et al. 2012). Such models suggest an antenna temperature increase of round about  $10\mu\text{K}$  in Q, V and W bands, while the V-band result is smaller, confirming the results in our table. This model also suggests that thermal dust emission will be most serious in the 150-GHz case and we will see similar and slightly higher  $\Delta T_A$  for future Planck and ACT data.

However, the discussion above did not consider the cluster SZ effect. If each cluster can offer a typical SZ signal of more than  $100\mu\text{K}$  antenna temperature decrease in the W band, the above effect can be neglected, yet the TD curves of optically selected clusters in Fig. 3 have shown the opposite result and negated this point. A possible conclusion is therefore that only a few clusters can offer a SZ signal (or most of them are very weak and can be covered by the radio-emission effect of galaxies). The reason may be simple: the ICM reaches high energy just after cluster formation and can then offer both thermal SZ effect and X-ray emis-

sion; however, such an effect cannot last for a long time-scale since the ICM is losing energy in a major way. This scenario clarifies why the SZ effect signal is apparently weaker than expected (Planck Collaboration. 2011a; Diego et al. 2003; P. Draper et al. 2012; Neelima Sehgal et al. 2013):

As regards SZ signal blind surveys or X-ray observations, these observe clusters that are able to offer a relative signal in the sky. With this selection effect, the observed samples are all within the ICM high-energy time-scale, so the detected cluster number will be small and the statistical result will show high SZ or X-ray signal, such as is the case for the TD curve of the Planck-189 sample in Fig. 3.

For optically selected galaxy clusters, the optical method gives a much more complete cluster sample, including a large percentage of clusters outside the ICM high-energy time-scale. In this case, the ICM of most clusters is not at high energy and its SZ signal is weak, so the main foreground effect can be covered by galaxy radio emission. We can thus see the  $\Delta T_A > 0$  effect in Fig. 3 and the lower  $Y_{500}$  signal for optically selected samples.

In conclusion, our model-independent method shows the main foreground effect of most (but not a few hundred) galaxy clusters directly (but not using the 1.4-GHz data imaging W-band result). The results of known SZ-signal-selected clusters and X-ray-observed clusters confirm the traditional thermal SZ result. Unexpectedly, however, the thermal SZ signal of most clusters in optically selected samples is contaminated (even covered) by something like radio emission. This may be the reason why the SZ signal detection result is lower than model expectations.

## ACKNOWLEDGMENTS

The authors sincerely thank Prof. Liu X.W.'s support in KIAA-PKU. The project is supported by Key Laboratory Opening Funding of Technology of Micro-Spacecraft (HIT.KLOF.2009098) and also by the development program for outstanding young teachers in HIT (BAQQ 92324501).

## REFERENCES

- Afshordi N., Lin Y.-T., Nagai D., Sanderson A. J. R., 2007, MNRAS, 378, 293
- Becker R. H., White R. L., Helfand D. J., 1995, ApJ, 450, 559.
- Bennett C. et al., arXiv:1212.5225
- Bielby R. M., Shanks T., 2007, MNRAS, 382, 1196
- Carlstrom J. E., Holder G. P., Reese E. D., 2002, ARA&A, 40, 643
- Carlstrom J. E. et al., 2011, PASP, 123, 568
- Delabrouille J., Cardoso J.-F., Le Jeune M., Betoule M., Fay G., Guilloux F., 2009, A&A, 493, 835
- Diego J. M., Silk J., Sliwa W., 2003, MNRAS, 346, 940
- Draper P., Dodelson S., Hao J., Rozo E., 2012, Phys. Rev. D, 85, 023005
- Gold B. et al., 2011, ApJS, 192, 15
- Hao J. et al., 2010, ApJS, 191, 254
- Holder G., Haiman Z., Mohr J. J., 2001, ApJ, 560, L111
- Koester B. P. et al., 2007, ApJ, 660, 239
- Kosowsky A. et al., 2006, New Astron. Rev., 50, 969

<sup>1</sup> <http://sundog.stsci.edu/first/catalogs.html>

Lieu R., Mittaz J. P. D., Zhang S.-N., 2006, ApJ, 648, 176  
Manera M., Mota D. F., 2006, MNRAS, 371, 1373  
Marrige T. A., 2011, ApJ, 737, 61  
Mehrtens N. et al., 2012, MNRAS, 423, 1024  
Melin J. B., Bartlett J. G., Delabrouille J., Arnaud M.,  
Piffaretti R., Pratt G. W., 2011, A&A, 525, A139  
Piffaretti R. et al., 2011, A&A, 534, A8  
Planck Collaboration. 2006,MNRAS, 369, 909  
Planck Collaboration.,2011a,A&A 536,A8.  
Planck Collaboration.,2011b,A&A 536,A10.  
Planck Collaboration.,2011c,A&A 536,A12.  
Sehgal N. et al., 2013, ApJ, 767, A38  
Sunyaev R. A., Zel'dovich Y. B., 1972, Comments Astro-  
phys. Space Phys., 4, 173  
Wen Z. L., Han J. L., Liu F. S., 2012, ApJS, 199, 34

This paper has been typeset from a  $\text{\TeX}$ / $\text{\LaTeX}$  file prepared  
by the author.